https://doi.org/10.17221/479/2025-PSE

The temperature sensitivity of stable organic carbon storage rises with increasing soil salinity

Chao Li[1], Yanling Tian[1], Wei He[2], Yanhong Lou[1], Hong Pan[1], Quangang Yang[1], Guoqing Hu[1], Yuping Zhuge[1,3], Hui Wang[1,3]**

[1]*National Engineering Research Center for Efficient Utilization of Soil and Fertilizer Resources, College of Resources and Environment, Shandong Agricultural University, Taian, P.R. China*
[2]*Observation and Research Station of Land Use Security in the Yellow River Delta, Ministry of Natural Resources (MNR), Shandong Provincial Territorial Spatial Ecological Restoration Center, Jinan, P.R. China*
[3]*National Center of Technology Innovation for Comprehensive Utilization of Saline-Alkali Land, Dongying, P.R. China*
**Corresponding authors: zhugeyp@sdau.edu.cn; huiwang@sdau.edu.cn*

Citation: Li C., Tian Y.L., He W., Lou Y.H., Pan H., Yang Q.G., Hu G.Q., Zhuge Y.P., Wang H. (2026): The temperature sensitivity of stable organic carbon storage rises with increasing soil salinity. Plant Soil Environ., 72: 16–27.

Abstract: Soil salinisation is a key determinant in soil fertility decline, exerting a direct negative impact on soil organic carbon. In the context of global warming, investigating the response mechanisms of soil organic carbon pools with varying salinity levels to climate change is essential for accurately assessing the carbon cycle and emission potential of degraded soils. Based on soil samples (B1–B6) collected along a coastal salinity gradient, indoor incubation experiments were conducted at 15 °C and 25 °C to characterise soil respiration and its temperature sensitivity (Q_{10}). Double-exponential models were used to simulate soil organic carbon (SOC) mineralisation, characterising active and stable organic carbon pools. The results demonstrated that the Q_{10} value of the stable organic carbon pool (7–8% of SOC mineralisation) was 103% higher than that of the active organic carbon pool (the initial 1% of SOC mineralisation). The Q_{10} value of the stable organic carbon pool was 32.6% higher at the high-salinity sites (B1, B2) than at the low-salinity sites (B4, B5). Soil organic carbon, total nitrogen (TN), and total salt (TS) were key regulators of Q_{10}. The Q_{10} of the active organic carbon pool correlated positively with SOC and TN but negatively with TS, whereas the stable pool showed the opposite trends. The stable organic carbon pool exhibits a salinity-amplified Q_{10}, implying that predictive models must account for this mechanism to avoid substantially underestimating carbon losses from degraded saline soils.

Keywords: coastal saline soil; SOC decomposition; terrestrial ecosystem; abiotic stress; carbon pool fractions

The soil carbon pool represents the largest carbon reservoir in terrestrial ecosystem. Globally, soil carbon storage is 2–3 times greater than the atmospheric carbon pool and more than double that of the terrestrial vegetation carbon pool (Davidson et al. 2000). Consequently, even minor fluctuations in soil carbon pools can significantly impact the entire terrestrial ecosystem. As the most active component of these pools, soil organic carbon (SOC) plays a critical role in determining soil fertility, productivity, and the global carbon cycle (Chen et al. 2025b). Based on the biological stability of SOC, it is commonly par-

Supported by the National Natural Science Foundation of China, Projects No. 42471069 and 42377313, and by the Modern Agriculture Industrial Technology Systems Project of Shandong Province, Project No. SDAIT-29-01.

© The authors. This work is licensed under a Creative Commons Attribution-NonCommercial 4.0 International (CC BY-NC 4.0).

https://doi.org/10.17221/479/2025-PSE

titioned into two or three distinct pools with varying turnover rates and activities, typically including an active organic carbon pool and a stable organic carbon pool. The active organic carbon pool consists of readily decomposable organic compounds characterised by higher solubility, availability, and ease of utilisation by plants and microorganisms, whereas the stable organic carbon pool comprises SOC stabilised through chemical and physical mechanisms, making it more resistant to the decomposition (Knorr et al. 2005).

Soil salinisation results from the upward accumulation of salts driven by evaporation and their downward redistribution by infiltration, which collectively determine salinity patterns and dynamic (Mavi et al. 2012). As a major cause of crop yield reduction, soil salinisation has become a key research focus in soil science in recent years (Qiu et al. 2025). In China, approximately 20% of cultivated land is affected by salinisation, exhibiting extensive and widespread distribution. This issue poses serious challenges to agricultural productivity and ecological stability nationwide. Soil salinity inhibits plant productivity, thereby reducing the input of soil organic matter (including organic carbon) and consequently diminishing SOC levels (Bhardwaj et al. 2019). Increased salinity lowers the osmotic potential of the soil solution, limiting water availability to soil organisms (Haj-Amor et al. 2022). Furthermore, high ionic concentrations may cause toxicity to soil microorganisms. Salinity also directly and/or indirectly influences microbial diversity and richness by altering soil properties (Chen et al. 2021). High salinity significantly depletes soil nutrients, potentially leading to reduced bacterial diversity. The response of soil microbial communities to salinity stress may further influence soil carbon cycling processes (Wang et al. 2025b).

Soil respiration serves as the primary pathway through which CO_2 fixed by terrestrial plants is released back into the atmosphere, making it a major driver of changes in SOC storage. However, the rate of SOC release is highly temperature-dependent (Schmidt et al. 2011). The temperature sensitivity of soil respiration (Q_{10}) refers to the factor by which soil respiration increases with a 10 °C rise in temperature. As a key parameter in terrestrial ecosystem carbon models, Q_{10} is widely used for predicting and interpolating soil respiration rates (Lin et al. 2015). Emerging evidence indicates that Q_{10} reflects not only the direct effect of temperature but also the integrated influence of moisture, substrate availability, and microbial activity (Davidson et al. 2000).

The temperature sensitivity of different carbon pools significantly contributes to uncertainties in climate change projections. Numerous studies have demonstrated that the Q_{10} value for carbon decomposition in the stable carbon pool is higher than that in the active pool (Lefèvre et al. 2014). This observation supports the Arrhenius kinetic theory, which posits that stable carbon, characterised by higher activation energy, exhibits greater Q_{10} compared to active carbon (Kätterer et al. 2011). However, other research has reported no significant differences in the temperature sensitivity responses between stable organic carbon pools and active carbon pools to temperature changes, showing similar responses under global warming scenarios (Fang et al. 2005). In other words, some studies suggest that active and stable organic carbon pools may have comparable temperature sensitivities.

Recent evidence suggests a positive correlation between Q_{10} of soil carbon decomposition and the degree of soil salinisation (Chen et al. 2025a). To validate this phenomenon, this study systematically examines the response patterns of temperature sensitivity in carbon decomposition across different salinity gradients, with particular focus on three key aspects: the differential characteristics of Q_{10} values between active and stable organic carbon pools during decomposition processes; the regulatory effect of soil salinisation intensity on Q_{10} values of carbon decomposition; and the identification of key environmental factors governing the temperature sensitivity of soil organic carbon decomposition.

MATERIAL AND METHODS

Soil sampling and characterisation. The study soil was collected from Wudi County, Binzhou City, Shandong Province (site details were shown in Table 1). The region features a temperate continental monsoon climate, with a mean annual temperature of 12.7 °C and an average annual precipitation of 564.8 mm. Geomorphologically, the area belongs to the Northwestern Shandong Floodplain of the North China Plain. The terrain slopes from higher elevations in the southwest to lower elevations in the northeast, with altitudes ranging between 1 and 8 m a.s.l. Soil samples were collected from the plow layer (0–20 cm) using the five-point sampling method. A total of six sampling sites (B1–B6) were established along a transect extending from northeast to southwest, with increasing distance from the coastline (B1 being

https://doi.org/10.17221/479/2025-PSE

Table 1. Site description and soil properties

	B1	B2	B3	B4	B5	B6
Site description						
Position	37°56'25.5"N, 117°57'06.3"E	37°56'15.3"N, 117°57'07.5"E	37°55'25.4"N, 117°56'15.1"E	37°55'04.7"N, 117°55'15.5"E	37°53'48.7"N, 117°53'28.4"E	37°46'16.2"N, 117°54'53.1"E
Elevation (m a.s.l.)	1	1	2	2	3	4
Vegetation	bare land	bare land	maize	maize	maize	maize
Soil properties						
$pH_{1:2.5}$	8.81	8.89	8.10	8.16	7.82	8.01
$TS_{1:5}$ (g/kg)	5.92	6.14	3.90	1.85	1.92	2.01
SOC (g/kg)	6.61	5.67	10.07	13.17	12.51	8.37
TN (g/kg)	0.66	0.63	1.08	1.28	1.27	0.93
AP (mg/kg)	34.0	31.0	55.7	37.1	7.3	24.4
AK (mg/kg)	840	1 000	699	742	415	251
Clay (%)	13.8	12.4	10.9	11.9	13.0	7.5
Microbial biomass (nmol PLFA/g)	10.25	10.30	28.61	32.75	23.67	24.04
B/F	4.96	6.20	4.08	4.24	4.50	3.81
G_+/G_-	0.67	0.83	0.83	0.84	1.00	0.86

Portions of the data were obtained from Chen et al. (2021). $TS_{1:5}$ – soil total salt at the soil-to-water ratio 1:5; SOC – soil organic carbon; TN – soil total nitrogen; AP – soil available phosphorus; AK – soil available potassium; PLFA – phospholipid fatty acid; B/F – bacteria-to-fungi ratio; G_+/G_- – PLFA biomass ratio of gram-positive bacteria to gram-negative bacteria

the closest and B6 the farthest). Consecutive sampling sites were spaced at least 2 km apart. At each site, a 20 m × 20 m quadrat was delineated, and five soil samples within the quadrat were collected diagonally, and homogeneously mixed. A portion was stored at 4 °C for future assessment of microbial properties, with the remainder air-dried for use in incubation experiments and for determination of soil chemical properties. Undisturbed soil samples were also taken to determine the field water holding capacity.

Experimental design. The experiment followed a completely randomised design with 12 treatments, comprising six soil salinity gradients (B1–B6) and two temperature gradients (15 °C and 25 °C). Each treatment was replicated four times, resulting in a total of 48 wide-mouth bottles. For each replicate, 50 g of soil was placed into a 500 mL wide-mouth bottle, and the soil moisture content was adjusted to 75% of the field water capacity for indoor incubation. The incubation was carried out in the dark using temperature-controlled incubators. A small plastic vial containing NaOH solution to absorb CO_2 was placed at the bottom of each wide-mouth bottle, which was then sealed. Soil respiration measurements were conducted at 0, 7, 14, 21, 28, 42, 56, 70, 91, 119, 147, 175, 210 and 255 days of the incubation. Throughout the incubation period, deionised water was replenished periodically to maintain constant soil moisture levels.

Determination of soil organic carbon mineralisation. Soil respiration rate was determined using the static alkali absorption method at regular intervals (Yim et al. 2002). The specific procedure was as follows: 10 mL of the CO_2-absorbed NaOH solution was pipetted, mixed with 5 mL of 1 mol/L $BaCl_2$ solution, and then 2 drops of phenolphthalein indicator were added. The mixture was titrated with 0.1 mol/L HCl solution (calibrated with borax before each titration) until the red color disappeared. The mineralisation amount of soil organic carbon during the incubation period was calculated based on the difference in HCl consumption between the control and treatment groups.

Analysis of soil basic physicochemical properties. Soil pH was measured in a suspension with a water-to-soil ratio of 2.5:1 (*v*/*m*) using a PHS-3C pH meter (INESA Scientific Instrument Co., Ltd., Shanghai, China). Total salt (TS) content was quantified by the gravimetric method. Total nitrogen (TN)

https://doi.org/10.17221/479/2025-PSE

content was measured with a Vario Macro cube elemental analyser (Elementar Analysensysteme GmbH, Langenselbold, Germany) (He et al. 2022). Determination of soil organic carbon (SOC) by potassium dichromate oxidation with external heating (Bhardwaj et al. 2019). The determination of available potassium (AK) content in soil was carried out using the alkali fusion-flame photometry method (Ramírez-Muñoz 1974). Soil available phosphorus (AP) contents were measured by the molybdenum-antimony anti-colourimetric method (Olsen and Sommers 1982). Following incubation, a portion of soil was immediately freeze-dried. Phospholipid fatty acids (PLFAs) were extracted from 5 g of freeze-dried soil using a chloroform:methanol:phosphate buffer (1:2:0.8) for 2 h. The extracts were separated into neutral lipids, glycolipids, and phospholipids *via* solid-phase extraction cartridges (silica gel) with sequential elution of chloroform, acetone, and methanol. The phospholipid fraction underwent mild alkaline methanolysis using a methanol:toluene (1:1) mixture and potassium hydroxide, incubated at 37 °C, followed by the addition of ultrapure water and acetic acid. Separation, quantification, and identification of fatty acid methyl esters were performed using an Agilent 6890 gas chromatograph equipped with a flame ionisation detector and an Ultra-2 column. Total PLFAs represented microbial biomass, and the bacteria-to-fungi ratio (B/F) reflected microbial community structure (Wang et al. 2013, 2014).

Data analysis. The first-order kinetic equation of soil organic carbon decomposition was adopted to determine the potential mineralisable organic carbon in the soil (Hartley and Ineson 2008):

$$C_{cum} = C_0 \times (1 - e^{-kt}) \quad (1)$$

Where: C_{cum} – cumulative release of CO_2 from the soil during a certain period of time, mg C/kg; C_0 – potential mineralisable organic carbon content, mg C/kg; k – decomposition rate of the organic carbon pool, 1/d; t – number of cultivation days, d.

The proportion of accumulated mineralisation of soil organic carbon was to determine the size and degradation rate of active organic carbon pool and stable organic carbon pool (Hartley and Ineson 2008):

$$y = C_a \times e^{-k\,1t} + C_b \times e^{-k\,2t} \quad (2)$$

Among them, y is the proportion of accumulated mineralisation of soil organic carbon; $C_a + C_b = 1$, where C_a and C_b – pool size of soil active organic carbon and stable organic carbon, respectively; k_1 and k_2 – decomposition rate constants of the active organic carbon pool and stable organic carbon pool, respectively; t – number of days of incubation.

The temperature sensitivity of active organic carbon and stable organic carbon was determined by the time required for the soil to mineralise a certain amount of carbon during incubation at 15 °C and 25 °C (Yang et al. 2025).

$$Q_{10} - q = t_{A-15}/t_{A-25} \text{ or } Q_{10}-q = t_{S-15}/t_{S-25} \quad (3)$$

Among them, Q_{10}–q is the temperature sensitivity of a certain component, t_{A-25} and t_{A-15} are the time required to release a certain amount of active organic carbon (usually 1% SOC) at 25 °C and 15 °C, respectively, and t_{S-25} and t_{S-15} are the time required to release a certain amount of stable organic carbon (usually 1% SOC) at 25 °C and 15 °C, respectively.

In this study, the Q_{10} of organic carbon pools was determined based on cumulative SOC mineralisation – the active pool represented by the initial 1% mineralisation, and the stable pool by 7–8% mineralisation. Based on the cumulative respiration intervals ranging from 1% to 8% of initial organic carbon, eight discrete Q_{10} values were derived for the six salinity levels and designated as Q_{10}–1^{st} to Q_{10}–8^{th}.

Statistical analysis and graph generation were performed using IBM SPSS 27 (IBM Corp., Armonk, USA) and Origin 2022 (Origin Lab Corporation, Northampton, USA). Before analysis, normal distribution and homogeneity of variance tests were conducted on the data. One way analysis of variance (ANOVA) was used to assess the differences in soil respiration and Q_{10}. Significant differences among treatments were further examined with post hoc least significant difference (*LSD*) tests at $P < 0.05$. Pearson correlation analysis was used to examine the relationship between Q_{10} of soil organic carbon mineralisation and soil properties. The first-order kinetic equation and double exponential model of soil organic matter mineralisation were constructed using R language (Auckland, New Zealand).

RESULTS

Soil organic matter mineralisation. At both incubation temperatures (15 °C and 25 °C), soil respiration rates decreased rapidly during the first week (Figure 1). The decline in soil respiration was consistently more pronounced at low-salinity sites (B4) than at high-salinity sites (B2), and was also greater at 15 °C compared to 25 °C. Under the higher temperature (25 °C), the reduction reached 36.94% at the site with

https://doi.org/10.17221/479/2025-PSE

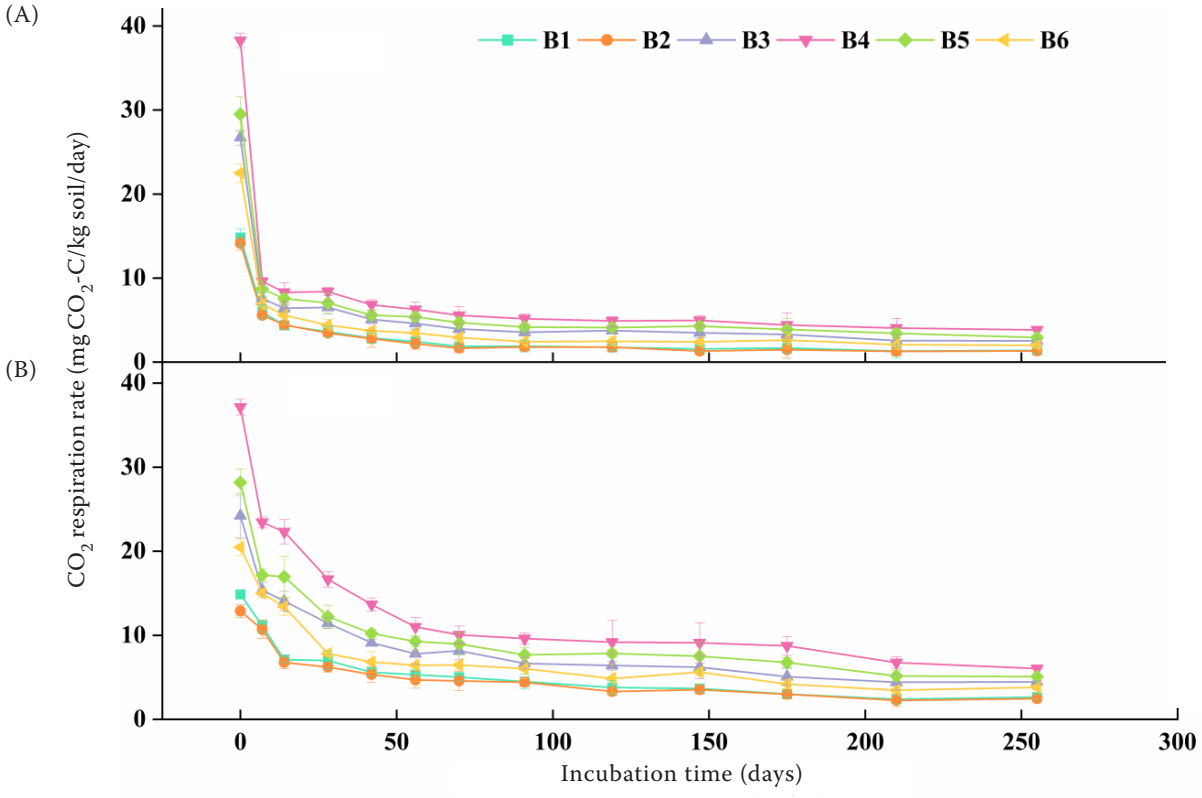

Figure 1. Respiration rates of soils with different salinisation at (A) 15 °C and (B) 25 °C

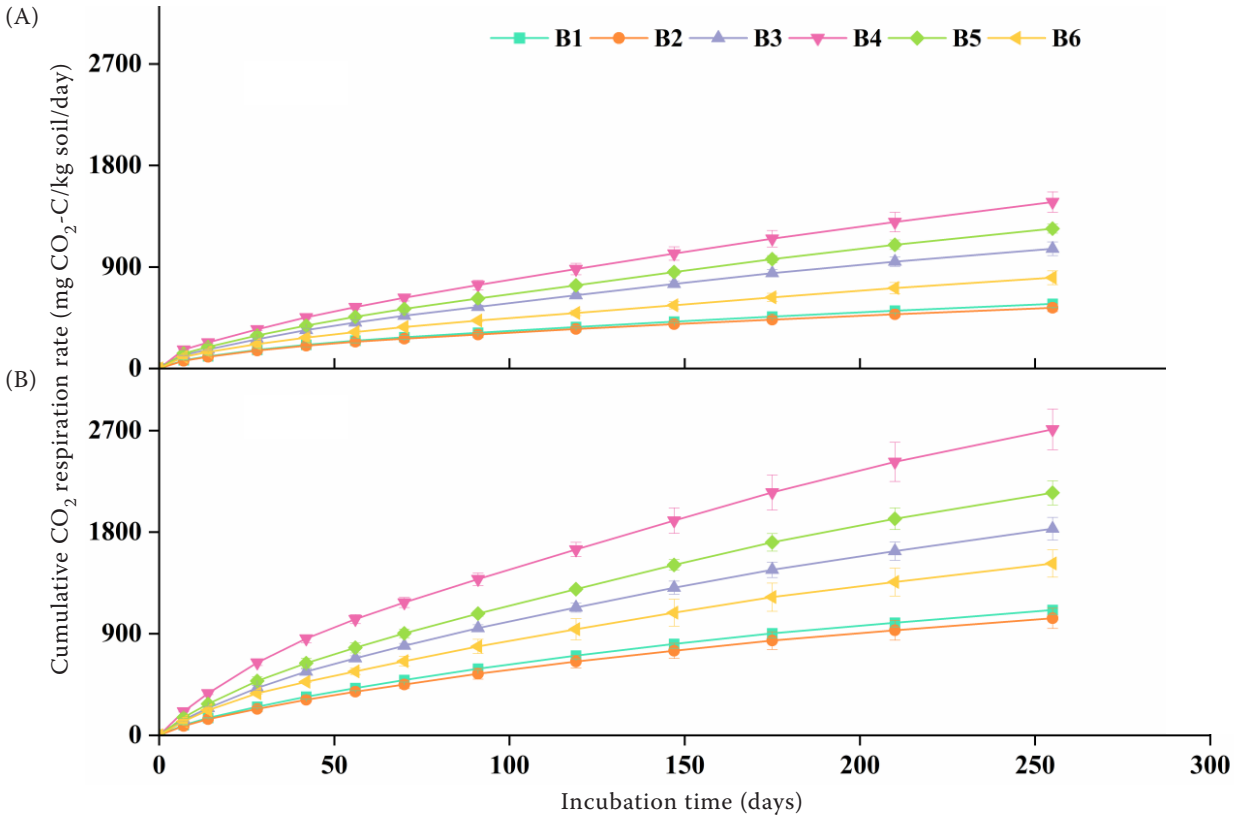

Figure 2. Cumulative CO_2 release from different saline soils at (A) 15 °C and (B) 25 °C

https://doi.org/10.17221/479/2025-PSE

the lowest total salt content (B4) and 17.00% at the site with the highest total salt content (B2). In contrast, under the lower temperature (15 °C), the decreases were more substantial, with values of 74.86% at B4 and 60.55% at B2 (Figure 1). Throughout the incubation period, cumulative CO_2 release was inversely correlated with soil salt content. At 25 °C, the total CO_2 emission from the lowest-salinity soil was 1.61 times that of the highest-salinity soil. Under 15 °C conditions, this ratio increased to 1.74 (Figure 2), further indicating that the inhibitory effect of salinity on carbon mineralisation is more evident at lower temperatures.

Soil carbon pool kinetics. The single-exponential model revealed significant temperature-induced variations in both the potential mineralisable carbon pool (C_0) and the decomposition rate constant (k) (Table 2). Site B4 exhibited the maximum C_0 value, with the 25 °C treatment showing a 45.53% higher value than the 15 °C treatment. Overall, C_0 was greater at the elevated temperature and exhibited a decreasing trend with increasing salinity. Conversely, the decomposition rate constant was lower at the higher temperature, resulting in correspondingly longer half-lives (Table 2). Analysis using the double-exponential model highlighted distinct temperature-dependent patterns in the composition and decomposition kinetics of active (C_a) and stable (C_b) organic carbon pools (Table 3). C_a was generally higher at 25 C, while C_b showed an opposite trend. The decomposition rate constant of the active organic carbon pool (k_1) was generally greater at the lower temperature, whereas k_2 values showed the reverse pattern and decreased with increasing salinity. Furthermore, the half-life of C_a was prolonged at the higher temperature, while that of C_b was shortened (Table 3).

Soil temperature sensitivity. The average Q_{10} of SOC decomposition exhibited a unimodal relationship with the cumulative proportion of respired C, peaking at 4–5% of the decomposed fraction (Figure 3). The Q_{10} value of the stable organic carbon pool (7–8% of SOC mineralisation) was 103% higher than that of the active organic carbon pool (the initial 1% of SOC mineralisation) (Figure 3). Furthermore, the Q_{10} value of the stable organic carbon pool was 32.6% higher at the high-salinity sites (B1, B2) than at the low-salinity sites (B4, B5). With the increase in the proportion of organic carbon respiration, Q_{10}

Table 2. Soil organic carbon decomposition parameters of the saline soils at different incubation temperatures using a single exponential model

Temperature	Site	C_0 (mg C/kg)	k (1/day × 10^{-3})	T1/2 of C_0 (day)
15 °C	B1	610.8 ± 37.6^{e}	9.08 ± 1.10^{a}	79.8 ± 9.7^{b}
	B2	570.9 ± 38.4^{e}	9.45 ± 1.30^{a}	78.0 ± 11.5^{b}
	B3	1 255.0 ± 50.1^{c}	6.71 ± 0.35^{b}	104.1 ± 4.9^{a}
	B4	1 801.5 ± 100.9^{a}	6.17 ± 0.33^{b}	113.5 ± 6.9^{a}
	B5	1 519.5 ± 33.8^{b}	6.07 ± 0.15^{b}	114.4 ± 2.9^{a}
	B6	891.9 ± 51.6^{d}	7.69 ± 0.54^{b}	91.4 ± 5.8^{ab}
25 °C	B1	1 340.6 ± 49.1^{d}	6.59 ± 0.30^{a}	106.0 ± 5.2^{a}
	B2	1 271.5 ± 81.4^{d}	6.39 ± 0.42^{a}	109.7 ± 6.5^{a}
	B3	2 251.0 ± 127.3^{c}	6.32 ± 0.49^{a}	111.6 ± 7.9^{a}
	B4	3 307.3 ± 210.6^{a}	6.36 ± 0.49^{a}	110.7 ± 7.8^{a}
	B5	2 802.8 ± 266.3^{b}	5.78 ± 0.61^{a}	125.3 ± 16.7^{a}
	B6	1 843.7 ± 125.6^{c}	6.47 ± 0.38^{a}	108.2 ± 6.1^{a}
Results (P-values) of two-way ANOVA				
Temperature		0.000	0.002	0.004
Site		0.000	0.010	0.016
Temp. × site		0.013	0.076	0.363

C_0 – potential mineralisable organic carbon content; k – decomposition rate of the organic carbon pool; T1/2 of C_0 – half-life of the initial pool of potential mineralisable organic carbon in soil

https://doi.org/10.17221/479/2025-PSE

Table 3. Soil organic carbon decomposition parameters of the saline soils at different incubation temperatures using a double exponential model

Temperature	Site	C_a (%)	k_1 (1/day × 10^{-2})	T1/2 of C_a (days)	C_b (%)	k_2 (1/day × 10^{-4})	T1/2 of C_b (days)
15°C	B1	2.56 ± 0.26^{ab}	4.87 ± 0.30^{a}	10.5 ± 0.9^{a}	97.44 ± 0.26^{ab}	2.59 ± 0.19^{d}	2 512.7 ± 163.6^{a}
	B2	3.18 ± 0.56^{a}	5.27 ± 1.46^{a}	12.6 ± 3.4^{a}	96.82 ± 0.56^{b}	2.67 ± 0.35^{cd}	2 476.2 ± 301.4^{a}
	B3	2.49 ± 0.21^{ab}	4.53 ± 0.57^{a}	10.5 ± 1.5^{a}	97.51 ± 0.21^{ab}	3.47 ± 0.19^{ab}	1 870.9 ± 97.4^{b}
	B4	2.33 ± 0.23^{ab}	5.62 ± 1.16^{a}	9.0 ± 1.6^{a}	97.67 ± 0.23^{ab}	3.80 ± 0.19^{a}	1 710.3 ± 74.4^{b}
	B5	2.06 ± 0.16^{b}	5.26 ± 0.89^{a}	9.1 ± 1.4^{a}	97.94 ± 0.16^{a}	3.35 ± 0.10^{ab}	1 952.0 ± 48.7^{b}
	B6	2.33 ± 0.09^{ab}	5.98 ± 0.64^{a}	8.6 ± 0.9^{a}	97.67 ± 0.09^{ab}	3.09 ± 0.19^{bcd}	2 116.5 ± 136.3^{ab}
25°C	B1	5.70 ± 0.52^{ab}	2.16 ± 0.28^{c}	20.1 ± 2.8^{ab}	94.30 ± 0.52^{ab}	5.04 ± 0.11^{c}	1 148.3 ± 15.1^{a}
	B2	6.48 ± 0.95^{a}	2.11 ± 0.42^{c}	21.5 ± 3.7^{a}	93.52 ± 0.95^{b}	5.42 ± 0.25^{bc}	1 044.1 ± 52.4^{ab}
	B3	5.16 ± 0.40^{ab}	2.48 ± 0.22^{c}	16.3 ± 1.5^{abc}	94.84 ± 0.40^{ab}	5.89 ± 0.35^{bc}	1 010.8 ± 50.0^{ab}
	B4	4.69 ± 0.38^{b}	3.61 ± 0.26^{ab}	11.4 ± 1.1^{c}	95.31 ± 0.38^{a}	7.30 ± 0.51^{a}	832.2 ± 51.7^{c}
	B5	4.29 ± 0.08^{b}	2.62 ± 0.32^{bc}	14.6 ± 0.9^{bc}	95.71 ± 0.08^{a}	5.79 ± 0.24^{bc}	1 054.2 ± 41.0^{ab}
	B6	4.19 ± 0.29^{b}	3.83 ± 0.54^{a}	11.2 ± 1.1^{c}	95.81 ± 0.29^{a}	6.39 ± 0.44^{ab}	967.3 ± 62.4^{bc}
Results (*P*-values) of two-way ANOVA							
Temp.		0.000	0.000	0.000	0.000	0.000	0.000
Site		0.003	0.229	0.005	0.003	0.000	0.000
Temp. × site		0.506	0.954	0.346	0.506	0.264	0.059

C_a – soil active organic carbon pool; C_b – soil stable organic carbon pool; k_1 – decomposition rate constant of the active organic carbon pool; k_2 – decomposition rate constant of the stable organic carbon pool; T1/2 of C_a – half-life of the initial pool of the soil active organic carbon pool; T1/2 of C_b – half-life of the initial pool of the soil stable organic carbon pool

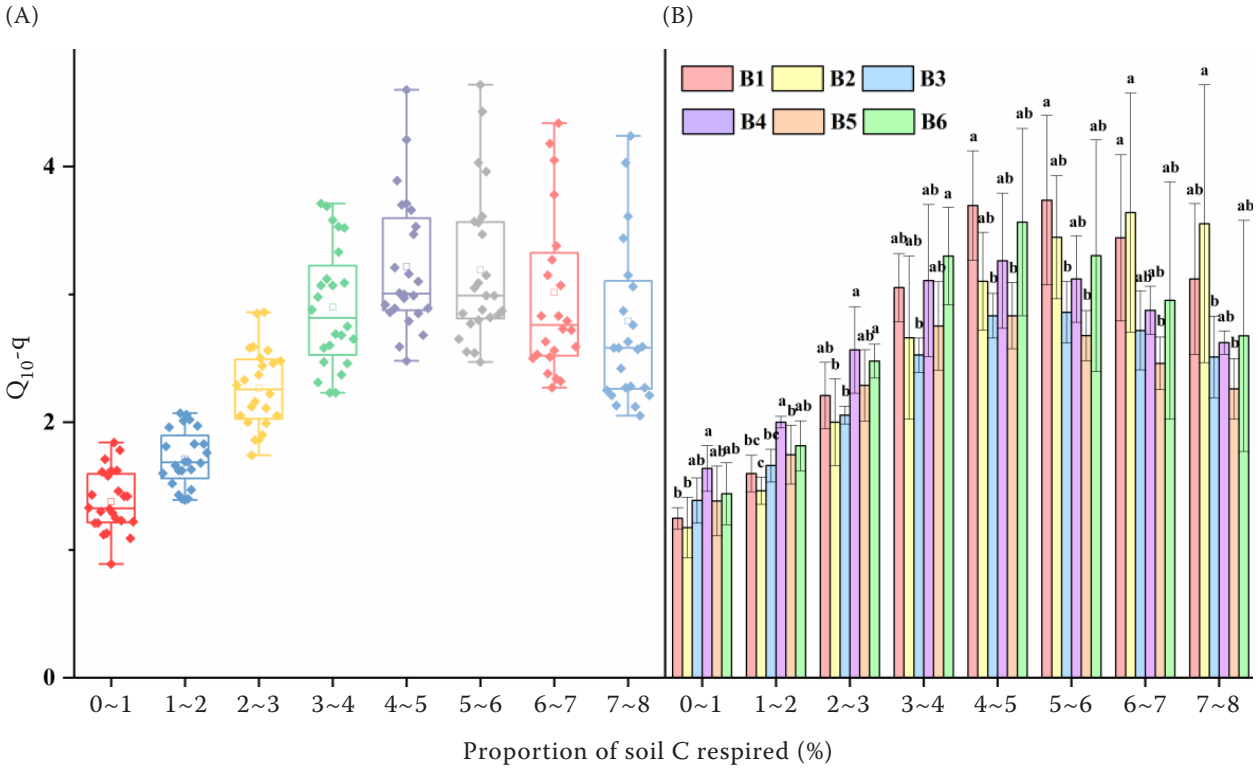

Figure 3. (A) Comparing Q_{10} from different organic carbon pools, and (B) changes in Q_{10} associated with the proportion of soil C respired in different coastal soils with different salinity levels

https://doi.org/10.17221/479/2025-PSE

showed a predominantly increasing trend, although there were significant differences among the different groups ($P < 0.05$). In the organic carbon respiration proportion ranges of 0–1% and 1–2%, the Q_{10} values of soils in low-salinity plots were higher than those in high-salinity plots. As the proportion of organic carbon respiration increased, when the proportion reached the 5–6% range, the differences among groups gradually became apparent, and the Q_{10} values of soils in high-salinity plots were significantly higher than those in other groups (Figure 3). This study demonstrated that the Q_{10} of the stable organic carbon pool in saline soils is higher than that of the active organic carbon pool.

Factors affecting temperature sensitivity. Correlation analysis revealed distinct relationships between soil temperature sensitivity and basic physicochemical properties (Figure 4). The Q_{10} of the active organic carbon pool showed significant positive correlations with SOC and TN contents, whereas the Q_{10} of the stable organic carbon pool was significantly negatively correlated with SOC. This indicates that higher SOC and TN contents enhance the temperature sensitivity of the active organic carbon pool but reduce that of the stable organic carbon pool. Furthermore, the Q_{10} of the active organic carbon pool was significantly negatively correlated with TS content, while the Q_{10} of the stable organic carbon pool demonstrated a significant positive correlation with TS. With increasing salinisation, the Q_{10} of the stable soil organic carbon pool becomes progressively higher, where soil organic matter and total salinity act as the principal drivers.

DISCUSSION

This study elucidated the mineralisation of soil organic carbon and the response of its temperature sensitivity to salinity gradients in coastal saline soils through incubation experiments at 15 °C and 25 °C. The results indicated that cumulative CO_2 release was significantly higher in the low-salinity soils (B4, B5 and B6) than in the high-salinity soils (B1 and B2), with the difference being more pronounced at

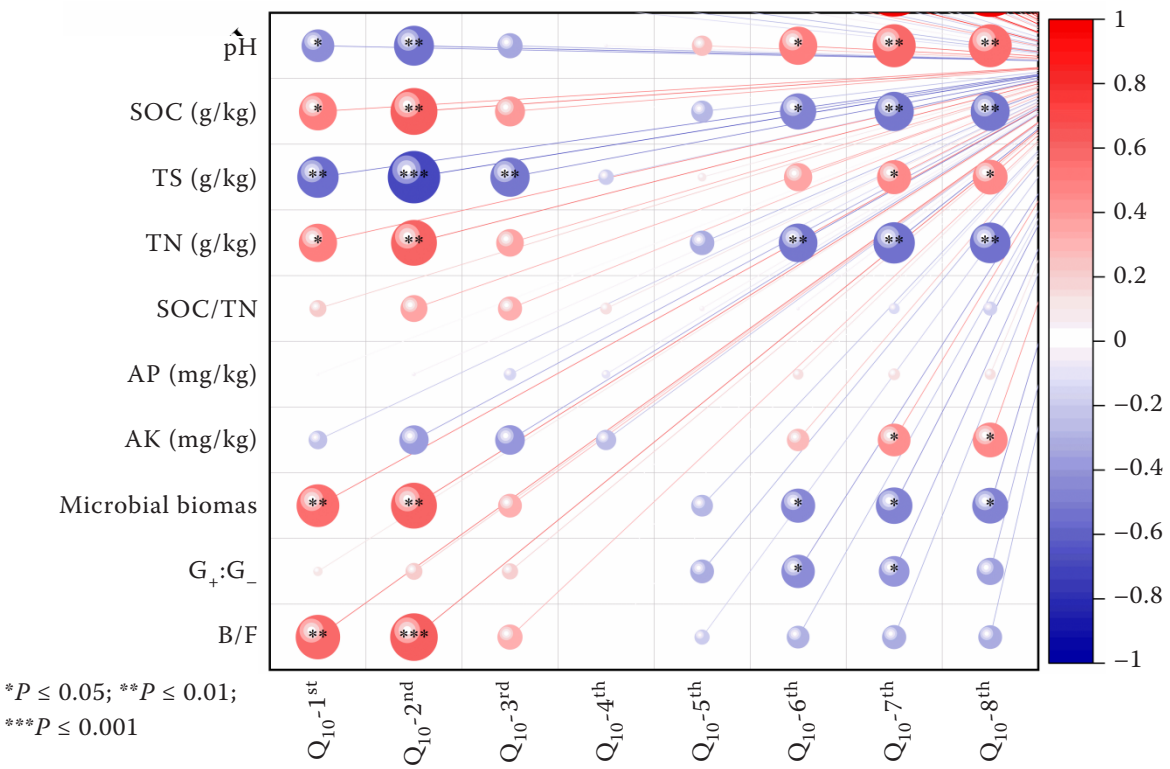

Figure 4. Correlations between temperature sensitivity of soil organic carbon (SOC) mineralisation and soil properties. Red lines denote positive correlations, while blue lines indicate negative correlations. TS – soil total salt; TN – soil total nitrogen; AP – soil available phosphorus; AK – soil available potassium; G_+/G_- – PLFA (phospholipid fatty acid) biomass ratio of gram-positive bacteria to gram-negative bacteria; B/F – bacteria-to-fungi ratio

https://doi.org/10.17221/479/2025-PSE

15 °C. These results demonstrate that the influence of temperature on soil respiration is modulated by soil salinity, with lower temperatures and lower salinity levels jointly leading to a more significant suppression of respiration rates. This observation is consistent with the classical understanding that salinity suppresses microbial activity and reduces the soil respiration rate (Guan et al. 2019, Yang et al. 2020).

Soil respiration Q_{10} serves as a critical parameter for evaluating the response of soil carbon cycling to global warming (Tarkhov et al. 2019). Based on the double-exponential model fitting of soil respiration data from laboratory incubation experiments, the active organic carbon pool was found to constitute 1.99–6.64% of total SOC, while the stable organic carbon pool formed the dominant fraction (Table 3). This is consistent with the research findings of Schütt et al. (2014). Our experimental results confirm that the Q_{10} of the stable organic carbon pool (represented by 7–8% SOC mineralisation) was 103% higher than that of the active organic carbon pool (represented by the initial 1% SOC mineralisation), with this difference increasing with elevated salinity (Figure 3). The temperature sensitivity of the active organic carbon pool was significantly positively correlated with soil organic carbon content, whereas the pool size itself was negatively correlated. During the active organic carbon pool-dominated phase (SOC mineralisation ratio < 3%), B2 exhibited significantly lower Q_{10} than B4. When the SOC mineralisation ratio reached > 4%, the Q_{10} at the high-salinity site tended to exceed that at the low-salinity site. The temperature sensitivity of the soil stable organic carbon pool generally exceeds that of the active organic carbon pool, consistent with previous findings (Xu et al. 2014). These findings support the Arrhenius-based kinetic theory proposed by Kätterer et al. (2011), confirming that the stable organic carbon pool possesses a higher activation energy and consequently a greater Q_{10} than the active organic carbon pool, while also refining the application of this theoretical framework in saline-alkali soils.

The regulatory effect of salinity on the temperature sensitivity of soil organic carbon pools exhibits a distinct characteristic that is dependent on the organic carbon pool. Soil salinity inhibited the temperature sensitivity of the active carbon pool but promoted that of the stable carbon pool. Salinisation does not uniformly amplify temperature sensitivity but exerts differential impacts on distinct organic carbon pools, potentially through modulation of microbial community structure (Yu et al. 2020). In this study, the reduced Q_{10} of the active organic carbon pool under high-salinity conditions may stem from impaired microbial activity due to salt stress, limiting its capacity to decompose labile carbon (Wang et al. 2021). Conversely, the increasing Q_{10} of the stable organic carbon pool with rising salinity is likely attributable to salinity-induced alterations in soil physicochemical properties, such as ionic composition and aggregate stability, which may enhance the decomposition efficiency or availability of recalcitrant organic matter (Ge et al. 2025). This differential response mechanism is presumably mediated through modifications in microbial community structure and function, thereby influencing the stability and turnover of soil carbon (Li et al. 2017). The elevated Q_{10} of the stable pool in saline soils may be further explained by the thermodynamic cost of microbial osmoregulation. Under salinity stress, microbes expend substantial energy to synthesise compatible solutes – a metabolic constraint that is particularly severe at lower temperatures. Warming relieves this energetic limitation, potentially leading to a disproportionately larger increase in microbial activity and thus a higher Q_{10}, consistent with thermodynamic theory (Schimel et al. 2007). Although our study did not directly measure microbial community dynamics, this osmoregulatory energy mechanism offers a plausible physiological explanation for the observed patterns. Notably, the double-exponential model employed here treats active and stable pools as independent entities. Therefore, potential interactions such as the priming effect – which salinity could further modulate – remain to be quantified in future isotopic studies.

Correlation and stepwise regression analyses indicated that SOC, TN, and TS are key regulators of Q_{10} (Figure 4). Both SOC and TN exhibited a highly significant positive correlation with Q_{10} of the active organic carbon pool and a highly significant negative correlation with Q_{10} of the stable organic carbon pool; TS showed the opposite trend. This regulatory mechanism reveals how soil properties indirectly modulate the temperature response of carbon decomposition through their effects on microbial substrate availability and metabolic activity (Li et al. 2020). This result not only challenges the traditional perception that the stable soil organic carbon pool is insensitive to environmental changes, but also highlights that when assessing the response

https://doi.org/10.17221/479/2025-PSE

of soil organic carbon pools in saline-alkali regions to climate warming, it is essential to comprehensively consider the synergistic regulatory effects of soil organic carbon, total nitrogen, and total salt, rather than focusing solely on a single factor (Rocci et al. 2021). Meanwhile, it also provides practical evidence for achieving the stability of soil organic carbon pools in these regions through the targeted improvement of soil physicochemical properties (e.g. moderate desalination, optimised carbon and nitrogen input). But the higher respiration rate and lower Q_{10} value observed at B6 may be partly attributable to its reduced physical protection capacity, rather than solely to its lower salinity level or pH value. This factor suggests that the observed salinity effect is, to some extent, a composite effect encompassing salinity, pH, soil texture, and associated changes in microbial habitat conditions. This study holds significant value in three dimensions, namely carbon cycle research under global warming, saline-alkali soil carbon pool management, and carbon cycle model optimisation (Wang et al. 2025a). The stable organic carbon pool, which constitutes the majority of the soil organic carbon stock (> 93% in this study), shows increasing Q_{10} with rising salinity. This implies that coastal saline soils may become significant carbon sources under the combined pressures of climate warming and soil salinisation. If the regulatory role of salinity on the Q_{10} of the stable organic carbon pool is overlooked in model projections, the carbon emission potential of saline regions may be substantially underestimated (Hassani et al. 2021). Therefore, the higher and salinity-amplified Q_{10} of the stable carbon pool suggests that its dominant role must be integrated into models to avoid underestimating the climate-carbon feedback in saline soils.

While this study provides valuable insights into how salinity regulates the temperature sensitivity of soil organic carbon pools, we note that several limitations should be considered. First, although laboratory incubation allows precise control of temperature and moisture, it cannot replicate field conditions. The use of air-dried and rewetted soils in the laboratory incubation for this study, while beneficial for controlling initial conditions, may introduce the "Birch effect". This could potentially lead to an overestimation of the active carbon pool size and affect the interpretation of its temperature sensitivity. Soil moisture fluctuations in the field can promote aggregate breakdown and reorganisation, altering carbon accessibility and potentially leading to Q_{10} responses that differ from those observed in the laboratory (Cruz-Paredes et al. 2021). Second, maintaining soils at 75% field capacity standardised volumetric water content but may not have equated physiological water availability across the salinity gradient, as high salt concentrations lower osmotic potential and could induce additional osmotic drought stress in saline treatments. Future studies controlling for soil water potential would help disentangle these interacting factors. Third, although microbial biomass was quantified *via* PLFA analysis, changes in microbial community structure and functional gene composition were not assessed. Limiting the identification of specific microbial taxa or functional genes associated with the observed Q_{10} differentiation (Chambers et al. 2016). Fourth, the estimated turnover time (> 2 000 days) for the stable carbon pool – derived from a 255-day incubation – carries inherent extrapolation uncertainty (equifinality). Thus, its associated Q_{10} should be interpreted cautiously for centennial-scale predictions (Sanderman et al. 2016). Moreover, these aerobic incubation results are primarily applicable to drained or intermittently dry coastal soils and may not be applicable to permanently waterlogged (anaerobic) environments.

It is worth noting that this study employed total salinity as the primary gradient. Variations in ionic composition (e.g., Na^+/Ca^{2+} ratio) and their distinct toxicities were not characterised, which may introduce additional complexity in interpreting salinity effects. Future studies isolating the specific impacts of individual ions would help clarify these mechanisms. The impact of soil salinisation on the temperature sensitivity of carbon storage is a complex systemic issue involving physical, chemical, and biological processes (Yu et al. 2020). Future research should adopt interdisciplinary approaches that integrate soil science, microbiology, and ecology to further elucidate the underlying mechanisms. Moreover, research outcomes should be translated into practical and scalable strategies for improving saline soils and managing carbon, thereby providing scientific support for mitigating global climate change and ensuring soil carbon security.

REFERENCES

Bhardwaj A.K., Mishra V.K., Singh A.K., Arora S., Srivastava S., Singh Y.P., Sharma D.K. (2019): Soil salinity and land use-land cover interactions with soil carbon in a salt-affected irrigation canal command of Indo-Gangetic plain. Catena, 180: 392–400.

https://doi.org/10.17221/479/2025-PSE

Chambers L.G., Guevara R., Boyer J.N., Troxler T.G., Davis S.E. (2016): Effects of salinity and inundation on microbial community structure and function in a mangrove peat soil. Wetlands, 36: 361–371.

Chen J., Wang H., Hu G., Li X., Dong Y., Zhuge Y., He H., Zhang X. (2021): Distinct accumulation of bacterial and fungal residues along a salinity gradient in coastal salt-affected soils. Soil Biology and Biochemistry, 158: 108266.

Chen M., Kuzyakov Y., Zhou J., Zamanian K., Wang S., Abdalla K., Wang J., Li X., Li H., Zhang H., Mganga K.Z., Li Y., Blagodatskaya E. (2025a): High soil salinity reduces straw decomposition but primes soil organic carbon loss. Soil Biology and Biochemistry, 207: 109835.

Chen Y., Kuzyakov Y., Ma Q., Du Z., Sun K., Xiao K., Liang X., Li Y., Zhang Y., Lai X., Fu W., Gao B., Wang F., Zhu S., Gao Q., Rillig M.C. (2025b): Aggregate size mediates the stability and temperature sensitivity of soil organic carbon in response to decadal biochar and straw amendments. Soil Biology and Biochemistry, 211: 109969.

Cruz-Paredes C., Tájmel D., Rousk J. (2021): Can moisture affect temperature dependences of microbial growth and respiration? Soil Biology and Biochemistry, 156: 108223.

Davidson E.A., Trumbore S.E., Amundson R. (2000): Soil warming and organic carbon content. Nature, 408: 789–790.

Fang C., Smith P., Moncrieff J.B., Smith J.U. (2005): Similar response of labile and resistant soil organic matter pools to changes in temperature. Nature, 433: 57–59.

Ge M., Xu H., Wang C., Sardans J., Peñuelas J., Wang W. (2025): Salinity decreases microaggregates organic carbon contribution in subtropical coastal wetland soil under the background of sea-level rise. Applied Soil Ecology, 213: 106317.

Guan C., Li X., Zhang P., Li C. (2019): Effect of global warming on soil respiration and cumulative carbon release in biocrust-dominated areas in the Tengger Desert, Northern China. Journal of Soils and Sediments, 19: 1161–1170.

Haj-Amor Z., Araya T., Kim D.-G., Bouri S., Lee J., Ghiloufi W., Yang Y., Kang H., Jhariya M.K., Banerjee A., Lal R. (2022): Soil salinity and its associated effects on soil microorganisms, greenhouse gas emissions, crop yield, biodiversity and desertification: a review. Science of The Total Environment, 843: 156946.

Hartley I.P., Ineson P. (2008): Substrate quality and the temperature sensitivity of soil organic matter decomposition. Soil Biology and Biochemistry, 40: 1567–1574.

Hassani A., Azapagic A., Shokri N. (2021): Global predictions of primary soil salinization under changing climate in the 21st century. Nature Communications, 12: 6663.

He W., Wang H., Ye W., Tian Y., Hu G., Lou Y., Pan H., Yang Q., Zhuge Y. (2022): Distinct stabilization characteristics of organic carbon in coastal salt-affected soils with different salinity under straw return management. Land Degradation and Development, 33: 2246–2257.

Kätterer T., Bolinder M.A., Andrén O., Kirchmann H., Menichetti L. (2011): Roots contribute more to refractory soil organic matter than above-ground crop residues, as revealed by a long-term field experiment. Agriculture, Ecosystems and Environment, 141: 184–192.

Knorr W., Prentice I.C., House J.I., Holland E.A. (2005): Long-term sensitivity of soil carbon turnover to warming. Nature, 433: 298–301.

Lefèvre R., Barré P., Moyano F.E., Christensen B.T., Bardoux G., Eglin T., Girardin C., Houot S., Kätterer T., van Oort F., Chenu C. (2014): Higher temperature sensitivity for stable than for labile soil organic carbon – evidence from incubations of long-term bare fallow soils. Global Change Biology, 20: 633–640.

Li J., Pei J., Cui J., Chen X., Li B., Nie M., Fang C. (2017): Carbon quality mediates the temperature sensitivity of soil organic carbon decomposition in managed ecosystems. Agriculture, Ecosystems and Environment, 250: 44–50.

Li J., Pei J., Pendall E., Fang C., Nie M. (2020): Spatial heterogeneity of temperature sensitivity of soil respiration: a global analysis of field observations. Soil Biology and Biochemistry, 141: 107675.

Lin J., Zhu B., Cheng W. (2015): Decadally cycling soil carbon is more sensitive to warming than faster-cycling soil carbon. Global Change Biology, 21: 4602–4612.

Mavi M.S., Marschner P., Chittleborough D.J., Cox J.W., Sanderman J. (2012): Salinity and sodicity affect soil respiration and dissolved organic matter dynamics differentially in soils varying in texture. Soil Biology and Biochemistry, 45: 8–13.

Olsen S.R., Sommers L.E. (1982): Phosphorus. In: Page A.L. (ed.): Methods of Soil Analysis Part 2 Chemical and Microbiological Properties. Madison, American Society of Agronomy, Soil Science Society of America, 403–430.

Qiu H.N., Yang S.H., Wang G.M., Zhang J., Dong S.D., Liu X.L., Xu Y., Liu H.W., Jiang Z.W., Meng T.Z., Zhang D.W. (2025): Projections of soil salinisation and organic carbon dynamics in the Yellow River Delta under future scenarios. Agricultural Water Management, 319: 109801.

Ramírez-Muñoz J. (1974): Chapter 22 – flame photometry. In: Richardson J.H., Peterson R.V. (eds.): Systematic Materials Analysis. New York, Academic Press, 85-123.

Rocci K.S., Lavallee J.M., Stewart C.E., Cotrufo M.F. (2021): Soil organic carbon response to global environmental change depends on its distribution between mineral-associated and particulate organic matter: a meta-analysis. Science of The Total Environment, 793: 148569.

Sanderman J., Baisden W.T., Fallon S. (2016): Redefining the inert organic carbon pool. Soil Biology and Biochemistry, 92: 149–152.

Schimel J., Balser T.C., Wallenstein M. (2007): Microbial stress-response physiology and its implications for ecosystem function. Ecology, 88: 1386–1394.

Schmidt M.W.I., Torn M.S., Abiven S., Dittmar T., Guggenberger G., Janssens I.A., Kleber M., Kögel-Knabner I., Lehmann J., Manning D.A.C., Nannipieri P., Rasse D.P., Weiner S., Trumbore S.E. (2011): Persistence of soil organic matter as an ecosystem property. Nature, 478: 49–56.

https://doi.org/10.17221/479/2025-PSE

Schütt M., Borken W., Spott O., Stange C.F., Matzner E. (2014): Temperature sensitivity of C and N mineralization in temperate forest soils at low temperatures. Soil Biology and Biochemistry, 69: 320–327.

Tarkhov M.O., Matyshak G.V., Ryzhova I.M., Goncharova O.Y., Bobrik A.A., Petrov D.G., Petrzhik N.M. (2019): Temperature sensitivity of soil respiration in palsa peatlands of the north of western Siberia. Eurasian Soil Science, 52: 945–953.

Wang B., Sun X., Yang Z., Li X., Yao B., Cai M., Sun T., Yang J., Han J., Zhang X., Jiang H. (2025a): Substrate chemistry trumps mineral protection in governing temperature sensitivity of organic carbon mineralization in saline lake sediments. Geochimica et Cosmochimica Acta, 407: 81–90.

Wang C., Morrissey E.M., Mau R.L., Hayer M., Piñeiro J., Mack M.C., Marks J.C., Bell S.L., Miller S.N., Schwartz E., Dijkstra P., Koch B.J., Stone B.W., Purcell A.M., Blazewicz S.J., Hofmockel K.S., Pett-Ridge J., Hungate B.A. (2021): The temperature sensitivity of soil: microbial biodiversity, growth, and carbon mineralization. The ISME Journal, 15: 2738–2747.

Wang Q., He T., Wang S., Liu L. (2013): Carbon input manipulation affects soil respiration and microbial community composition in a subtropical coniferous forest. Agricultural and Forest Meteorology, 178–179: 152–160.

Wang Q., Wang S., He T., Liu L., Wu J. (2014): Response of organic carbon mineralization and microbial community to leaf litter and nutrient additions in subtropical forest soils. Soil Biology and Biochemistry, 71: 13–20.

Wang Z., Xia S., Bolan N., Li Q., Zhu Z., Yu B., Yang W., Fan Y., Bian R., Liu X., Zheng J. (2025b): Elevated salinity decreases soil multifunctionality by driving bacterial community structure and network complexity. Science of The Total Environment, 1000: 180362.

Xu W., Li W., Jiang P., Wang H., Bai E. (2014): Distinct temperature sensitivity of soil carbon decomposition in forest organic layer and mineral soil. Scientific Reports, 4: 6512.

Yang C., Wang X., Miao F., Li Z., Tang W., Sun J. (2020): Assessing the effect of soil salinization on soil microbial respiration and diversities under incubation conditions. Applied Soil Ecology, 155: 103671.

Yang Z., Hu J., Chen X., Zhang Y., Wang Y., Peng J., Fei J., Luo G., Liao C. (2025): Intercropping-driven effects on soil organic carbon mineralization and its temperature sensitivity are associated with soil C-N-P stoichiometry and carbon-acquiring microorganisms and enzymes. Geoderma, 460: 117411.

Yim M.H., Joo S.J., Nakane K. (2002): Comparison of field methods for measuring soil respiration: a static alkali absorption method and two dynamic closed chamber methods. Forest Ecology and Management, 170: 189–197.

Yu Y., Li X., Zhao C., Zheng N., Jia H., Yao H. (2020): Soil salinity changes the temperature sensitivity of soil carbon dioxide and nitrous oxide emissions. Catena, 195: 104912.

Received: October 23, 2025
Accepted: December 29, 2025
Published online: January 21, 2026